Article:

Liu, Xudong, Bouxin, Florent P., Fan, Jiajun orcid.org/0000-0003-3721-5745 et al. (4 more authors) (2021) Effect of metal triflates on the microwave-assisted catalytic hydrogenolysis of birch wood lignin to monophenolic compounds. INDUSTRIAL CROPS AND PRODUCTS. 113515. ISSN 0926-6690

https://doi.org/10.1016/j.indcrop.2021.113515

Effect of metal triflates on the microwave-assisted catalytic hydrogenolysis of birch wood lignin to monophenolic compounds

Xudong Liu,[ab] Florent P. Bouxin,[b*] Jiajun Fan,[b] Richard Gammons,[b] Vitaliy L. Budarin,[b] Changwei Hu,[a*] James H. Clark[b]

[a] *Key Laboratory of Green Chemistry and Technology, Ministry of Education, College of Chemistry, Sichuan University, Chengdu 610064, China*

[b] *Green Chemistry Centre of Excellence, Department of Chemistry, University of York, Heslington, York YO10 5DD, UK*

*Corresponding authors

E-*mail addresses*: florent.bouxin@york.ac.uk; changweihu@scu.edu.cn.

Abstract

The lignin-first biorefinery strategy could produce bio-based phenols from the extraction and depolymerization of native lignin in lignocellulosic biomass. Herein, we report an effective Lewis acid-promoted delignification and production of monophenolic compounds in birch sawdust assisted by microwave heating without external hydrogen for the first time. The screening of different metal triflates revealed that $Fe(OTf)_3$ was best for the delignification and depolymerization of birch sawdust. Without the addition of a Lewis acid, the yield of monophenolic compounds was 10.5 wt% (based on the lignin content in birch sawdust), while it increased significantly to 32.9 wt% with the addition of $Fe(OTf)_3$ (0.0276 g) under the identical conditions (190 ^{o}C, 1 h), which demonstrated the catalytic C-O-C bond scission promoted by $Fe(OTf)_3$. Simultaneously, the delignification degree also rose sharply from 32.6 wt%

to 47.5 wt%. This work demonstrated the efficient $Fe(OTf)_3$-induced delignification and depolymerization of lignin in birch sawdust to obtain a high yield of monophenolic compounds without external hydrogen assisted by microwave heating, representing a novel advance in the “lignin-first” biorefinery field.

Keywords: Lignin, Birch, Microwave, Metal triflates, Monophenolic compounds

1. Introduction

The depletion of fossil resources and increasingly deteriorating environment have driven us to exploit and explore the valorization of lignocellulosic biomass (Li et al., 2017; Liao et al., 2020; Shuai et al., 2016; Sun et al., 2018; Yan et al., 2020). Due to the enormous research efforts made to utilize the carbohydrates (cellulose and hemicellulose); the value of lignin has been underestimated over the past few decades (Ragauskas et al., 2014; Rinaldi et al., 2016; Schutyser et al., 2018). The worldwide paper industry generates approximately 50 million tons of lignin wastes annually, with the majority incinerated to supply heat, thereby causing severe global environmental issues (Cederholm et al., 2020; Haq et al., 2020; Wang et al., 2019b; Zhou et al., 2020). Therefore, developing a biorefinery strategy for the efficient valorization of lignin seems essential and significant in terms of sustainable development and economic viability (Li et al., 2015; Renders et al., 2017; Renders et al., 2019). Lignin is a complex aromatic polymer biosynthesised by the radical polymerization of three monolignols units (p-coumaryl, coniferyl and sinapyl alcohol), which are randomly-linked by various C-O-C (β-O-4, α-O-4, 4-O-5) and C-C (β-β, 5-5, β-5) linkages (Cao et al., 2020; Liu et al., 2020b; Shen et al., 2020; Wong et al., 2020). The efficient depolymerization of lignin to obtain well-defined phenolic chemicals faced great difficulties and obstacles due to its structural heterogeneity and rigidity (Liu et al., 2019; Wang et al., 2019a; Xu et al., 2014).

Recently, a reductive depolymerization strategy proposed by the Abu-Omar's and Sels' groups has emerged aiming at maximizing the yield of monophenolic compounds while retaining carbohydrates in the pulp via a one-pot method (Bosch et al., 2015; Parsell et al., 2015). During this process, solvo-thermal extraction of lignin fragments, subsequent catalytic depolymerization and further stabilization of monophenolic compounds and lignin-derived oligomers to avoid undesirable condensation reactions were achieved (Abu-Omar et al., 2021; Cooreman et al., 2020). An appreciable yield of monophenolic compounds could be obtained at the expense of longer reaction time (4-8 h) and higher reaction temperature (200-260 ^{o}C), which is an energy-consuming chemical process (Liu et al., 2020b; Liu et al., 2020c; Van den Bosch et al., 2017). Therefore, exploiting an energy-saving and cost-effective method for the fractionation and depolymerization of lignin in raw biomass could promote the development of "lignin-first" biorefinery (Chen et al., 2020b). In order to achieve an efficient delignification and depolymerization of lignin, cheap and readily available Lewis acids (metal chlorides, metal acetates, metal triflates) were commonly added to accelerate the release of lignin fragments via the cleavage of ester and ether bonds between lignin and hemicellulose (Deuss and Barta, 2016; Huang et al., 2016; Jastrzebski et al., 2016; Klein et al., 2016; Shu et al., 2018).

In 2015, Shu et al. investigated the roles of various metal chlorides for the liquefaction of lignin and observed that the highest yield (28.5 wt%) of monophenolic compounds was obtained with $CrCl_3$ used under harsh conditions (260 ^oC, 5 h) (Shu et al., 2015). The promoting effect of Cl^- in Lewis acid could be ascribed to its hydrogen bond acceptor and polarization reagent for C-O bonds in lignin. However, the metal chlorides were unstable and susceptible to form some complexes in water, such as $[Cr(OH)(H_2O)_5]^{2+}$ and $[Al(OH)_2(H_2O)_5]^+$ (Tang et al., 2015; Yunden et al., 2019). Therefore, metal triflates which served as more promising water-tolerant Lewis acids for the delignification and depolymerization of lignin were recently investigated (Deuss et al., 2016; Deuss et al., 2017; Huang et al., 2016; Jastrzebski et al., 2016). In 2016, Jastrzebski et al. found that the yield of monophenolic compounds increased from 2.6 wt% to 12.1 wt% when $Sc(OTf)_3$ was added with propenyl guaiacol and propenyl syringol being the major products (Jastrzebski et al., 2016). The distribution of monophenolic compounds demonstrated that a weak Lewis acid with lower loading could favour the formation of propenyl-substituted phenols via a reductive mechanism. In the same year, Deuss et al. achieved the highest monomer yield (19.3 wt%) with $Fe(OTf)_3$ added, and acetal monophenolic compounds were formed as the predominant products via the aldol reaction upon β-O-4 bond cleavage (Deuss et al., 2016). Recently, Huang et al. achieved higher yield (42 wt%) of monophenolic compounds than previous literatures over Pd/C with Al (III)-triflate as co-catalyst when 30 bar of H_2 was added (Huang et al., 2017). However, the high pressure of hydrogen was dangerous and the transportation and storage of hydrogen is expensive. Except for utilizing lignin in biomass, Wang et al. achieved near theoretical yields of hydrocarbons from lignin model compounds by the combined catalysis of $Hf(OTf)_4$ and ruthenium-based catalysts (Ru/C and Ru/Al_2O_3) (Wang et al., 2018).

In our previous work, 28.6 wt% and 36.9 wt% yield of monophenolic compounds were obtained without the addition of Lewis acid or external hydrogen at 190 °C for 3 h and 6 h, whereas the longer reaction time proved harmful for the lifespan of the magnetron in the microwave reactor (Liu et al., 2020a). Herein, a highly efficient delignification and depolymerization of lignin in birch sawdust with the help of metal triflates assisted by microwave heating utilizing a hydrogen-free strategy is reported.

2. Experimental

2.1 Feedstock and materials

Birch wood sawdust was obtained from Weihua Manufacturing Factory in Guangdong Province, China. The birch sawdust with the particle size between 40 and 80 meshes was used in this work, which was composed of 37.7 wt% of cellulose (determined as glucan), 16.6 wt % of hemicellulose (determined as xylan, arabinan and galactan), and 23.3 wt% of Klason lignin (acid insoluble lignin). 5 wt% Pt/C catalyst was purchased from Sigma-Aldrich. Methanol (MeOH, HPLC grade), dichloromethane (DCM, HPLC grade) and all monophenolic compounds of analytic grade (AR) were obtained from commercial suppliers and used as received. $Sc(OTf)_3$ (98%), $Ce(OTf)_3$ (98%) and $Cu(OTf)_2$ (98%) of analytic grade were purchased from Alfa Aesar, while other metal triflates [$Yb(OTf)_3$ (99.99%), $Mg(OTf)_2$ (97%), $Ca(OTf)_2$ (99.9%), $Zn(OTf)_2$ (98%), $Fe(OTf)_2$ (⩾85%) and $Fe(OTf)_3$ (90%)] were purchased from Sigma Aldrich and used without further purification.

Table 1. Comparison of previous literatures and this work for the depolymerization of lignin using Lewis acid.

Feedstock	Solvent	T (°C)	t (h)	Gas/ pressure	Catalysts	Lewis acids (mmol/L)	Monomer yield (wt%)	Delignification (wt%)	Carbohydrates retention	Ref.
Alkali lignin	MeOH	260	5	40 bar H_2	5 wt% Pd/C	$CrCl_3$ (12.5)	28.5	80.7	-	(Shu et al., 2015)
Poplar dioxasolv lignin	Dioxane/H_2O (9/1)	175	2	-	$[Rh(cod)Cl]_2$	$Sc(OTf)_3$ (1.36)	12.1	-	-	(Jastrzebski et al., 2016)
Walnut methanosolv lignin	Dioxane	140	1/4	1.0 atm	-	$Fe(OTf)_3$ (23)	19.3	-	-	(Deuss et al., 2016)
Birch sawdust	MeOH	180	2	30 bar H_2	5 wt% Pd/C	$Al(OTf)_3$ (0.8)	45	80.8	Glucan 96.6 Xylan 44.5	(Huang et al., 2017)
Birch sawdust	H_2O/MeOH (3:7, v/v)	190	1	1.0 atm	5 wt% Pt/C	$Fe(OTf)_3$ (1.37)	32.9	47.5	Glucan 83.0 Xylan 40.4	This work

2.2 *Catalytic depolymerization of lignin*

Microwave-assisted catalytic depolymerization of lignin was performed in a microwave instrument (flexiWAVE, Milestone). The experiments were conducted in batches using 100 mL PTFE vessels, which were initially loaded with 0.1 g 5 wt% Pt/C,

1.0 g birch sawdust, 0.055 mmol metal triflates and 40 mL H_2O/MeOH (3:7, v/v) co-solvent. Herein, the variety and amount of catalysts, the kind and ratio of co-solvents were directly selected from the optimized conditions in our previous work (Liu et al., 2020a). Stirring was fixed at 40% of the stirring power, which allowed maintaining the catalyst in suspension and avoided external mass-transfer limitations. The temperature ramp was set as 15 min, to allow the reaction mixtures to reach the reaction temperature (190 ^{o}C), which was then maintained for 1 h. The conventional heating was conducted in a 100 mL stainless vessel using Parr reactor and the other procedures were similar to those using microwave heating. During the reaction, system pressure rose up to 24.8 bar within the fluctuation range of 1.0 bar. Each reaction was conducted in duplicate. Upon completion of the pretreatment, the reaction mixture was vacuum filtrated and washed with H_2O/MeOH (3:7, v/v) solution until the filtrate was clear. The washed solid residue was then dried in an oven at 105 ^{o}C overnight for further compositional analysis. Part of the liquid fraction was extracted by DCM to analyse monophenolic compounds, while the rest were kept for HPLC analysis.

2.3 *Quantitative analysis of monophenolic compounds*

The monophenolic compounds in DCM phase were quantified using internal standard method on a Hewlett Packard GC 6890 equipped with Restek Rxi-5HT (30 m, 0.25 mm, 0.25 μm film thickness) column and flame ionisation detector. The oven temperature program started at 60 °C for 1 min and increased up to 340 °C at 8 °C min^{-1}. Injector and detector temperatures were set at 340 and 350 °C, respectively. The benzyl alcohol was used as an internal standard. The yield of monophenolic compounds was calculated by the equation:

$$\text{Yield of monophenolic compounds (wt\%)} = \frac{\text{weight of monophenolic compounds (g)}}{\text{weight of lignin in birch sawdust (g)}} \times 100 \quad (1)$$

2.4 Quantitative analysis of sugar-derived products

The monosaccharides (glucose, xylose, arabinose/rhamnose), organic acids (lactic acid, acetic acid, formic acid, levulinic acid), levoglucosan (LGA), 5-hydroxymethylfurfural (HMF) and furfural (FF) in the liquid products were quantified using an Agilent 1260 Infinity HPLC system (USA) equipped with a Agilent HiPlex H (300 × 7.7 mm, 8 μm particle size) column. Samples (5 μL) were eluted at 0.4 mL min^{-1} using a mobile phase of 5 mM H_2SO_4. The column and refractive index detector temperatures were set at 60 °C and 55 °C, respectively. The yield of sugar-derived products was calculated based on the following equation:

$$\text{Yield of sugar-derived products (wt\%)} = \frac{\text{weight of sugar-derived products (g)}}{\text{weight of carbohydrates in birch sawdust (g)}} \times 100 \quad (2)$$

2.5 Composition analysis of birch sawdust and reaction residues

The biomass was acid hydrolyzed by mixing 100 mg of the sample with 1 mL of 72%

H_2SO_4 in a serum bottle and keeping it at 40 °C for 2 hours, followed by the addition of 28 mL water for a second-stage hydrolysis and heating to 121 °C in an autoclave for another 1 hour. After cooling down to the ambient temperature, the solution was filtered. The acid insoluble ash was measured by combusting the acid insoluble residue in a furnace with the ramp temperature program heated up to 500 °C (10 °C/min, 6 h). The Klason lignin content was determined by deducing the acid insoluble ash from acid insoluble residue content. The content of each sugar (glucose, xylose, arabinose and rhamnose), organic acids (formic acid, acetic acid) and sugar-derived products (HMF, FF) were determined by HPLC analysis of the hydrolyzate (filtrate phase). The solid residue yield and delignification degree were calculated according to the following equations:

$$\text{Solid residue yield (wt\%)} = \frac{\text{weight of solid residue (g)}}{\text{weight of birch sawdust (g)}} \times 100 \qquad (3)$$

$$\text{Delignification (wt\%)} = \frac{\text{content of lignin in birch sawdust (wt\%)} - \text{content of lignin in solid residue (wt\%)} \times \text{solid residue yield}}{\text{content of lignin in birch sawdust (wt\%)}} \qquad (4)$$

3. Results and Discussion

3.1 Screening of the metal triflates

The screening of different metal triflates for the distribution and yield of monophenolic compounds was shown in Fig. 1 and Fig. S1. Overall, compared with the control reaction (without metal triflates), $Yb(OTf)_3$, $Mg(OTf)_2$, $Ce(OTf)_3$, $Sc(OTf)_3$ catalyzed liquid products exhibited a lower yield, while the other metal triflates showed a promoted yield of monophenolic compounds, which could be possibly ascribed to the different Lewis acidity (electron-acceptor ability) of the metal triflates. Among all the metal triflates applied, the highest yield of monophenolic compounds (32.9 wt%) was achieved for $Fe(OTf)_3$, including 9.3 wt% yield of 4-propyl syringol (S2) and 12.8 wt% yield of 4-propenyl syringol (S4) (Table S1). In 2016, Deuss et al. compared the effect of three metal triflates [$Bi(OTf)_3$, $Fe(OTf)_3$, $Hf(OTf)_4$] on the depolymerization of methanosolv lignin and observed that $Fe(OTf)_3$ showed higher yield than the other triflates. The results of this work agree well with the literature (Deuss et al., 2016).

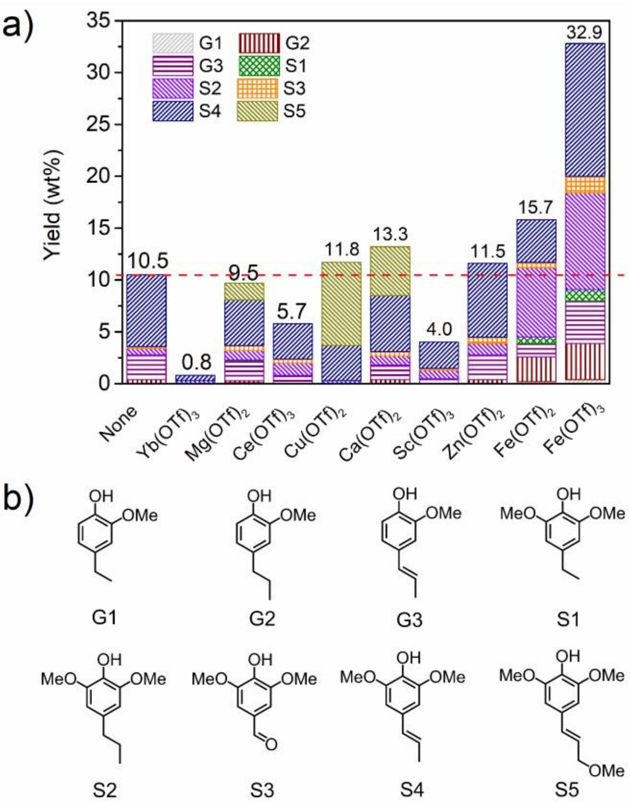

Fig. 1 (a) The yield and distribution of monophenolic compounds as a function of various metal triflates; (b) chemical structures of detected monophenolic compounds. Reaction conditions: 1.0 g birch sawdust, H_2O/MeOH (3:7, v/v; 40 mL), 0.1 g 5% Pt/C, 0.055 mmol metal triflates, 190 ^{o}C, 1 h.

In terms of the distribution of propenyl and propyl-substituted phenols, 4-proyl guaiacol (G2) and S2 were the major products for $Fe(OTf)_2$, while 4-propenyl guaiacol (G3) and S4 were the dominated monomers for all the other metal triflates. The overall distribution of monophenolic compounds demonstrated that syringol-derived monophenolic compounds were the dominant products while guaiacol-type phenols were in a much lower yield, which was in agreement with the fact that hardwood (birch sawdust) lignin was principally composed of S (syringol) units with a smaller quantity of G (guaiacol) units (Sun et al., 2019). Except for the predominant unsaturated propenyl and saturated propyl substituted phenols, γ-OH methylated propenyl syringol (S5) was observed for $Mg(OTf)_2$, $Cu(OTf)_2$ and $Ca(OTf)_2$. Besides, a minor quantity of ethyl substituted guaiacol (G1) and syringol (S1) was obtained in the liquid products with $Mg(OTf)_2$, $Fe(OTf)_2$ and $Fe(OTf)_3$ used. Deuss et al. also reported that ethyl- and ethanol-substituted phenolics could be obtained from the hydrogenation/dehydration of C2-aldehydes in the reaction system with HOTf followed by the addition of Ru/C and H_2. Our work using Pt/C and in-situ H_2 from methanol agrees well with previous literatures (Deuss et al., 2017; Deuss et al., 2015; Liu et al., 2020a).

In order to specify the different role of metal triflates and Pt/C catalyst, several control experiments as a function of $Fe(OTf)_3$ and Pt/C catalyst were conducted (Fig. S2). For the liquid products obtained without Pt/C catalyst, S5 could be observed regardless of the metal triflates, however, the peak assigned to S5 disappeared when Pt/C was added, which implied the catalytic hydrogenolysis/hydrolysis of γ-ether bond (Liu et al., 2020a). When no $Fe(OTf)_3$ was added (Table 2), the yield of monophenolic compounds increased from 6.4 wt% to 10.5 wt% with Pt/C . However, the yield of monophenolic compounds increased dramatically to 32.9 wt% when both $Fe(OTf)_3$ and Pt/C were added, which demonstrated the synergistic effect of Lewis acid $Fe(OTf)_3$ and noble metal catalyst Pt/C for the delignification and depolymerization of lignin to produce monophenolic compounds. However, the yield of monophenolic compounds dropped sharply to 20.1 wt% under identical conditions using conventional heating (Fig. S3). The comparative yield (32.7 wt%) could be achieved by conventional heating while longer reaction time (2 h for conventional vs 1 h for microwave) was required, which further highlighted the higher efficiency and promoting effect of microwave heating. Similarly, Kumar et al. utilized microwave heating to achieve an equivalent yield compared with conventional heating while requiring less energy and time (Kumar et al., 2019). Besides, the selectivity toward saturated propyl-substituted phenolics (G2 and S2) was enhanced from 0 to 9.5% when Pt/C was added, and further increased to 38.9% when $Fe(OTf)_3$ was used, which demonstrated the depolymerization of extracted lignin fragments promoted by $Fe(OTf)_3$ and further side-chain hydrogenation of produced unsaturated monophenolic compounds.

Table 2. The yield of monophenolic compounds as a function of $Fe(OTf)_3$ and Pt/C.

Metal triflates	Cat.	Monomer yield (wt%)									Selec.(G2+S2) (%)
		G1	G2	G3	S1	S2	S3	S4	S5	Total	
None	None	-	-	-	-	-	-	2.2	4.2	6.4±0.5	-
None	Pt/C	-	0.4	2.4	-	0.6	0.2	6.9	-	10.5±0.9	9.5
$Fe(OTf)_3$	None	-	-	-	-	-	0.8	1.2	5.2	7.2±0.8	-
$Fe(OTf)_3$	Pt/C	0.4	3.5	4.1	1.1	9.3	1.6	12.8	-	32.9±1.1	38.9

Reaction condition: 1.0 g birch sawdust, 0.0276 g $Fe(OTf)_3$, $H_2O/MeOH$ (3/7, v/v, 40 mL), 5 wt% Pt/C (0.1 g), 190 ^{o}C, 1 h.

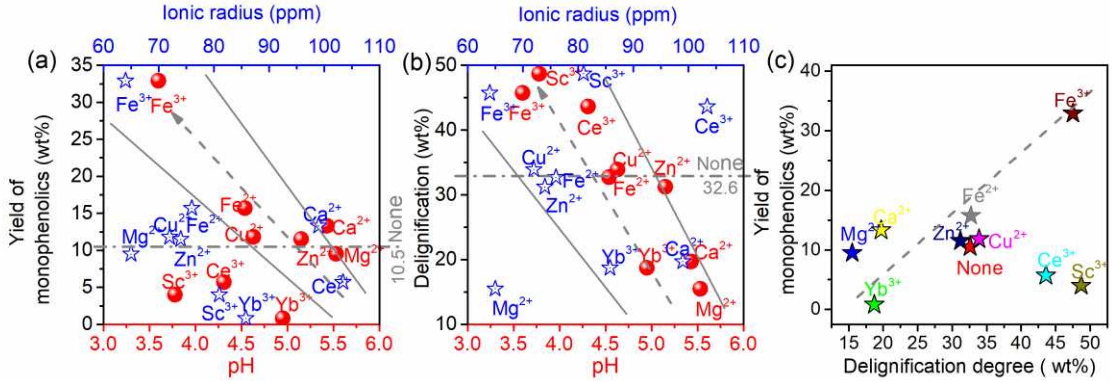

Fig. 2 Correlation between (a) yield of monophenolic compounds, (b) delignification and the medium pH/ the ionic radius of metal ions; (c) yield of monophenolic compounds and delignification degree.

In order to further elucidate the difference of metal triflates, the correlation between delignification/yield of monophenolic compounds and medium pH/ionic radius of metal ions is shown in Fig. 2. When comparing the correlation between yield of monophenolic compounds and solution pH/metal ionic radius (Fig. 2a), an obvious correlation between the yield of monophenolics and medium acidity was observed except for Ce^{3+} and Sc^{3+}. The exception of Ce^{3+} and Sc^{3+} could be possibly explained by the condensation reactions which was highly promoted in the more acidic conditions (Shuai and Saha, 2017).

As shown in Fig. 2b, there was a much clearer correlation between delignification and medium pH/ionic radius. The Fe^{3+}, Sc^{3+}, Ce^{3+} triflates solutions showed a medium pH of 3.60, 3.78, 4.31 from the hydrolysis of metal triflates, which corresponded to a higher delignification degree (47.5, 48.7, 43.6 wt%) (Table 3). Overall, the delignification degree increased with the decrease of the radius of metal ions and medium pH of metal triflates solution. During the delignification process, metal triflates participated in the cleavage of ester and ether bonds between lignin and carbohydrates (Lignin-carbohydrates complexes, LCC) as well as partial cracking of the β-O-4 ether bonds of lignin, thereby liberating lignin-derived oligomeric fragments from raw lignocellulosic biomass (Huang et al., 2017; Huang et al., 2016).

Lewis acids promoted the rupture of ester and ether bonds via the nucleophilic substitution, thereby the metal ions with a smaller ionic radius were more likely to attack the ester and ether bonds. In terms of the monophenolic yield, Fe^{3+} exhibited the highest yield of 32.9 wt%, which could be possibly ascribed to its smaller ionic radius (64 pm) with higher charge density and stronger electrostatic force, thereby favouring the attack of intermolecular ester and ether bonds between lignin and carbohydrates as well as intramolecular ether linkages of lignin (Yu et al., 2016; Zhao et al., 2019).

As shown in Fig. 2c, a good correlation between the monophenolic yields and delignification except for Ce^{3+} and Sc^{3+} was observed. For Ce^{3+} and Sc^{3+}, high acid strength of those metal triflates solution could increase lignin recondensation during the delignification process, thereby negatively impacting the subsequent hydrogenolysis yields of monophenolics (Lan and Luterbacher, 2019a; Shuai and Saha, 2017). This explanation was also highlighted in Fig. 2a, showing the importance between the yields of monophenolic and medium acidity (also exception for Ce^{3+} and Sc^{3+}).

Table 3. The effect of metal ions on the medium pH, ionic radius, yield of monophenolic compounds and delignification.

Metal ions	pH	Ionic radius (pm)	Yield of monophenolics (wt%)	Delignification (wt%)
None	-	-	10.5±0.9	32.6±1.6
Yb^{3+}	4.95	85.8	0.8±0.2	18.7±2.9
Mg^{2+}	5.53	65	9.5±0.9	15.5±2.3
Ce^{3+}	4.31	103.4	5.7±0.6	43.6±1.0
Cu^{2+}	4.63	72	11.8±1.2	33.9±1.0
Ca^{2+}	5.43	99	13.3±0.8	19.7±4.1
Sc^{3+}	3.78	81	4.0±0.5	48.7±2.4
Zn^{2+}	5.15	74	11.5±0.3	31.2±0.8
Fe^{2+}	4.54	76	15.7±0.8	32.7±0.6

Fe^{3+}	3.60	64	32.9±1.1	47.5±0.1

3.2 Optimization of the Fe(III)-triflate loading

As shown in Fig. 3 and Fig. S4, the effect of $Fe(OTf)_3$ loading on the yield and distribution of monophenolic compounds was also investigated. The total yield of monophenolic compounds increased from 10.5 wt% to 21.5 wt% when the loading of $Fe(OTf)_3$ was increased from 0 g to 0.0138 g, and the highest yield of 32.9 wt% was achieved with a $Fe(OTf)_3$ loading of 0.0276 g (Table S2). When the loading of $Fe(OTf)_3$ further increased up to 0.1104 g, the yield of monophenolic compounds continually dropped to 4.3 wt%. As suggested by Marks et al., the metal triflates mediated C-O bond scission/hydrogenolysis was the rate-determining step in the tandem catalytic process following a first-order with respect to substrate and the concentration of metal triflates (Assary et al., 2013; Atesin et al., 2012). To conclude, a proper loading of $Fe(OTf)_3$ could contribute to the efficient release and extraction of lignin fragments from lignocellulosic matrix, while high loading of Lewis acid $Fe(OTf)_3$ could promote the condensation reactions of lignin fragments via the nucleophile attack of benzylic carbocation, thereby lowering the yield of monophenolic compounds (Lan and Luterbacher, 2019b).

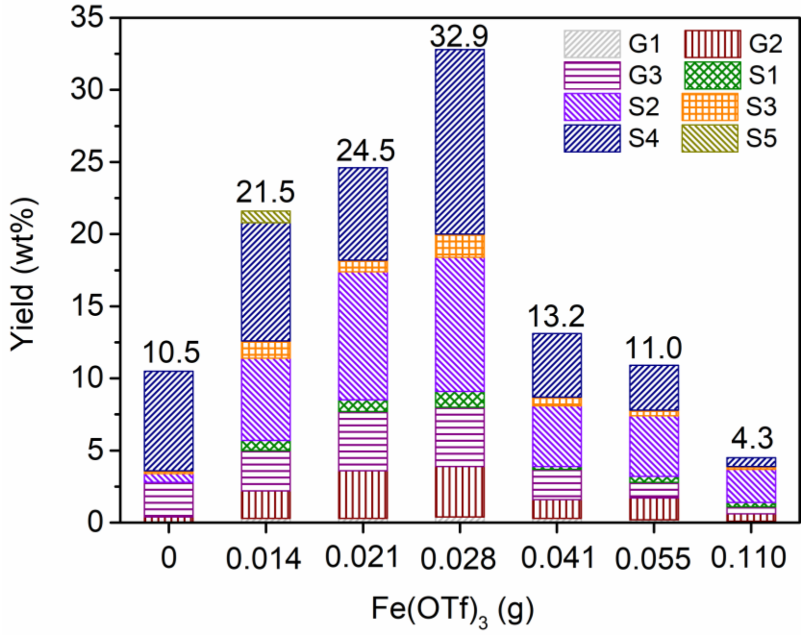

Fig. 3 The effect of loading of $Fe(OTf)_3$ on the yield and distribution of monophenolic compounds.

3.3 Sugar-derived products

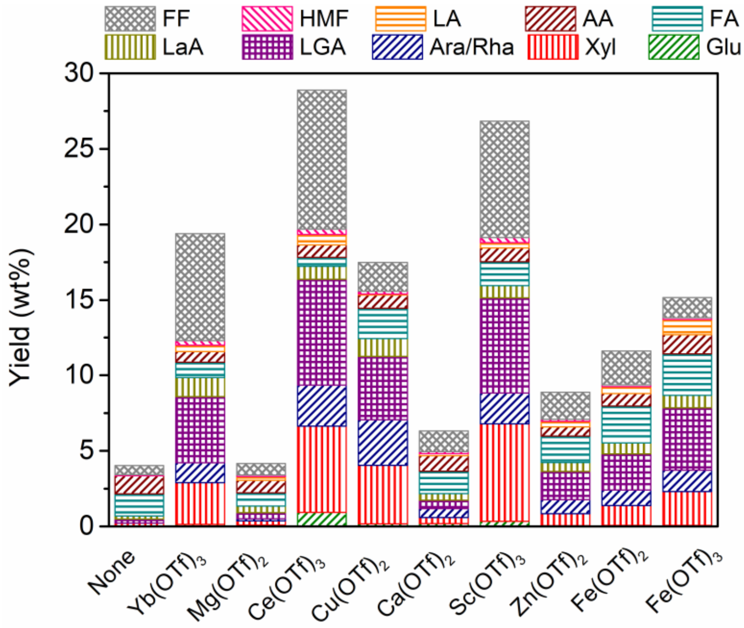

Fig. 4 The effect of different metal triflates on the distribution and yield of sugar-derived products. Glu: Glucose; Xyl: Xylose; Ara/Rha: Arabinose/Rhamnose; LGA: Levoglucosan; LaA: Lactic Acid; FA: Formic acid; AA: Acetic acid; LA: Levulinic acid; HMF: 5-hydroxymethylfurfural; FF: Furfural.

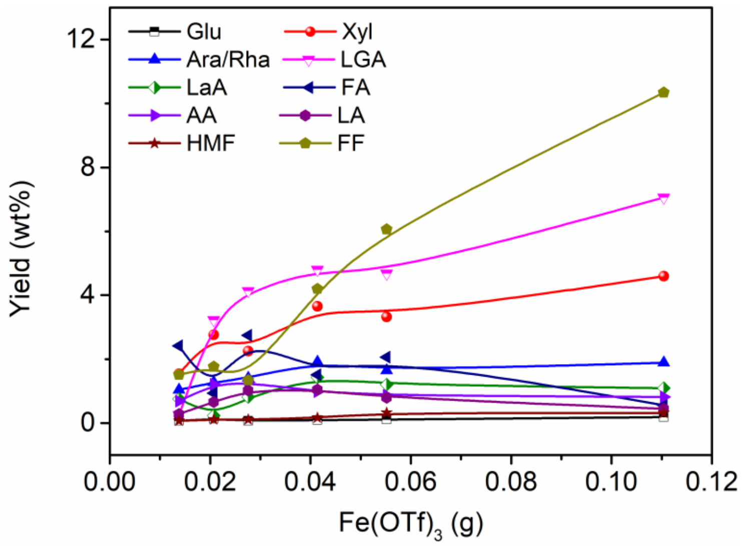

Fig. 5 The effect of Fe(OTf)$_3$ loading on the yield of sugar-derived products.

The sugar-derived products, including monosaccharides (glucose/Glu, xylose/Xyl, arabinose/rhamnose), organic acids (lactic acid/LaA, formic acid/FA, acetic acid/AA, levulinic acid/LA), aldehydes (5-hydroxymethyl furfural/HMF, furfural/FF) and levoglucosan (LGA); were analysed to better understand the dissolution behavior of cellulose and hemicellulose. Without the addition of metal triflates, 4.0 wt% yield of sugar-derived products was achieved with FA (1.5 wt%) and AA (1.2 wt%) being the major products (Fig. 4). The highest total yield (28.9 wt%) of these sugar-derived products was obtained for Ce(OTf)$_3$, with furfural (9.2 wt%), LGA (7.0 wt%) and xylose (5.7 wt%) being the major products (Table S3). Besides, a minor quantity of glucose, HMF and organic acids were also detected. The lowest yield of sugar-derived products was observed for Mg(OTf)$_2$, which could be possibly explained by the difference of medium pH of metal triflates solutions [Ce(OTf)$_3$, pH=4.31; Mg(OTf)$_2$, pH=5.53; see Table 2]. As for Fe(OTf)$_3$, LGA, FA and Xyl were the dominated products.

LGA was significantly enhanced when the metal triflates were added with the exception of weaker Lewis acids [$Mg(OTf)_2$; $Ca(OTf)_2$], which could be ascribed to the acid-induced dehydration of glucose (Bouxin et al., 2019; Chen et al., 2020a; Zhao et al., 2018). The highest yield (6.5 wt%) of Xyl was achieved for $Sc(OTf)_3$ (pH=3.78), with a high yield of LGA (6.3 wt%) and FF (7.7 wt%). To conclude, the metal triflates solutions [$Ce(OTf)_3$, $Sc(OTf)_3$] with higher Lewis acidity (lower medium pH) can significantly favour the formation of Xyl, LGA and FF due to acid-induced dehydration reactions.

The effect of $Fe(OTf)_3$ loading on the yield and distribution of sugar-derived products was also investigated, as shown in Fig. 5. The total yield of sugar-derived products increased from 8.6 wt% to 27.3 wt% when the loading of $Fe(OTf)_3$ rose from 0.014 g to 0.110 g (Table S4). The dominant products, Xyl, Ara/Rha, LGA and FF showed an upward trend with higher loading of $Fe(OTf)_3$. While Glu, organic acids (LaA, FA, AA, LA) and HMF hovered around at a relatively lower yield. To summarize, higher loading of $Fe(OTf)_3$ could promote the dehydration of glucose and xylose to produce LGA and FF, respectively.

3.4 The fate of carbohydrates in the reaction residue.

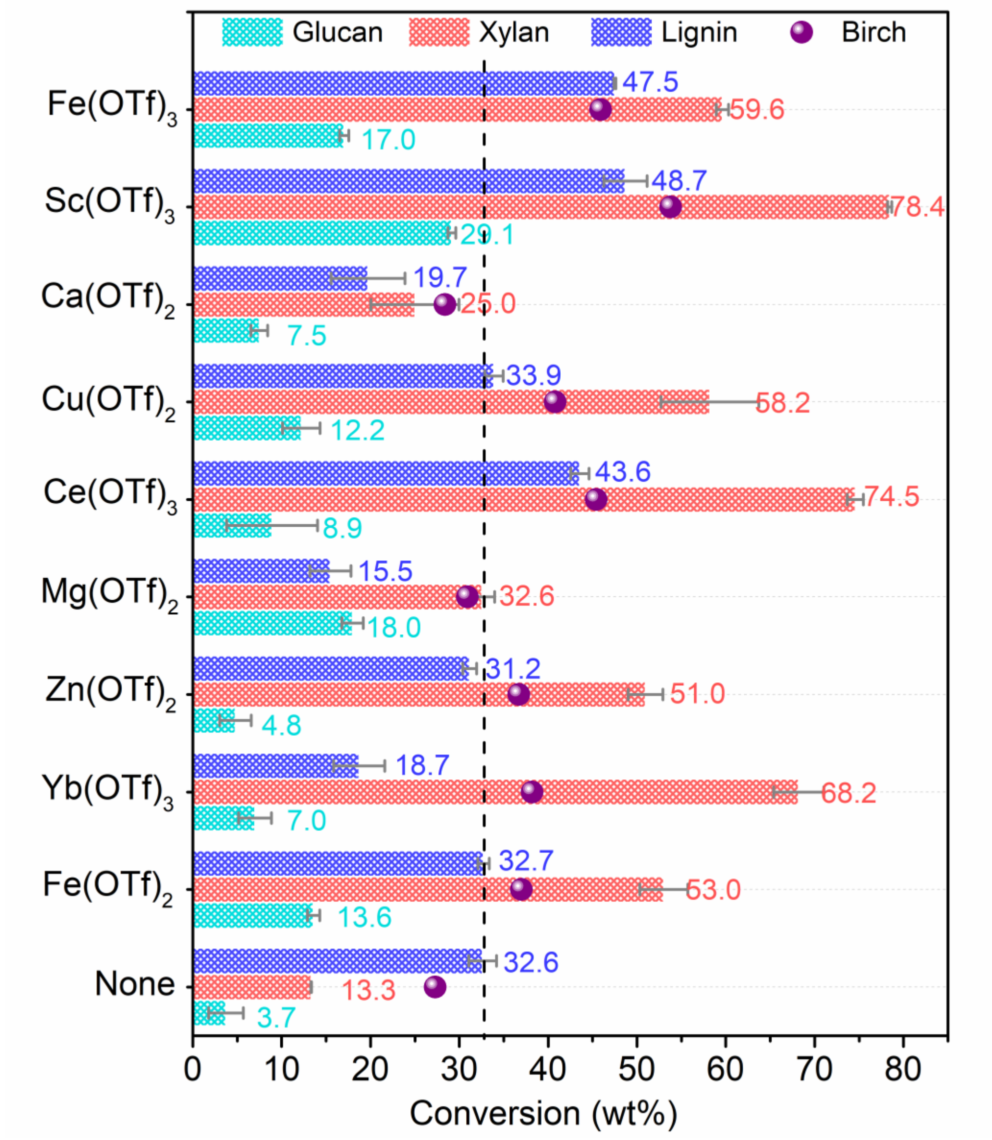

Fig. 6 The effect of different metal triflates on the conversion of birch sawdust and the three main components.

The effect of various metal triflates on the conversion of birch sawdust and the three main components are shown in Fig. 6. The highest conversion (53.8 wt%) of birch sawdust was observed for Sc(OTf)$_3$, with 29.1 wt%, 78.4 wt% and 48.7 wt% conversion of glucan, xylan and lignin, respectively (Table S5). Higher conversion of xylan and lignin could be achieved for Ce(OTf)$_3$, Sc(OTf)$_3$ and Fe(OTf)$_3$, which indicated the cleavage of intramolecular linkages between lignin and hemicellulose (lignin-carbohydrates complexes, LCC) during solvo-thermal extraction (Huang et al., 2016; Liu et al., 2019). The conversion of glucan fluctuated below 20 wt% except for Sc(OTf)$_3$. Ca(OTf)$_2$, Mg(OTf)$_2$ solution with higher pH value (5.43, 5.53) corresponded to a lower conversion of birch sawdust (28.4 wt%, 30.9 wt%). 45.9 wt% conversion of birch sawdust and 47.5wt% conversion of lignin was obtained for Fe(OTf)$_3$. To conclude, the addition of metal triflates exerted a major influence on the conversion of lignin and hemicellulose, which accords well with previously reported work (Huang et al., 2017).

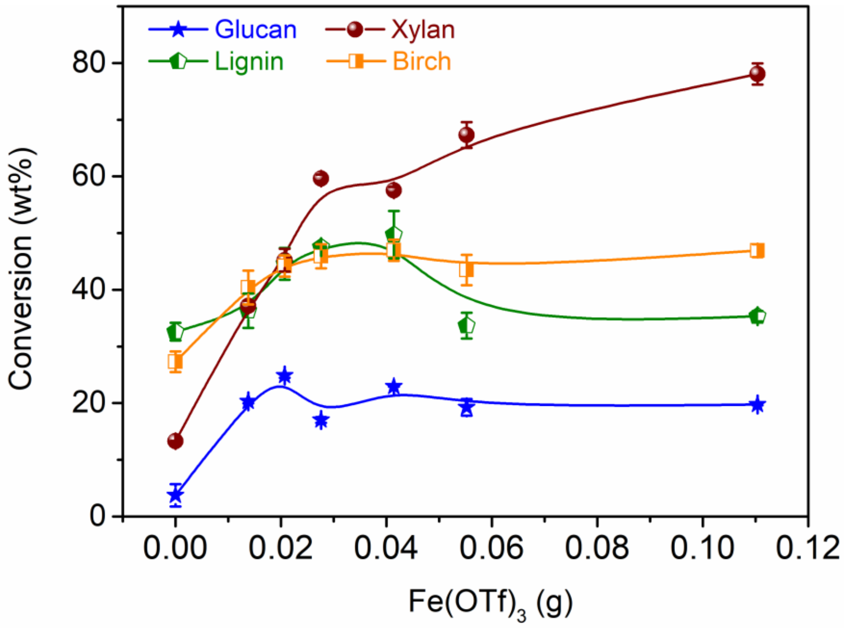

Fig. 7 The effect of Fe(OTf)$_3$ loading on the conversion of birch sawdust and three main components.

Fig. 7 showed the conversion of birch sawdust and the three components as a function of loading of Fe(OTf)$_3$. The conversion of birch sawdust increased from 27.3 wt% to 47.0 wt% as the loading of Fe(OTf)$_3$ was increased from 0 g to 0.0414 g, and stabilized around 47.0 wt% with further increasing of the loading (Table S6). Accordingly, the conversion of xylan and lignin also increased significantly from 13.3 wt% to 57.5 wt% and 32.6 wt% to 49.7 wt%, respectively. The different trends for the dissolution behavior between xylan and lignin was that the conversion of xylan continuously increased to 78.1 wt% with a loading of 0.1104 g, while the conversion of lignin conversely reduced to 35.3 wt% possibly due to the condensation reactions of low-molecular weight oligomers at a higher loading of Lewis acid. The conversion of glucan showed a distinct trend as a function of $Fe(OTf)_3$ loading, which increased from 3.7 wt% to 20.3 wt% as the loading rose from 0 g to 0.0138 g and levelled off around 20 wt% with the further addition of $Fe(OTf)_3$. To conclude, a proper loading of $Fe(OTf)_3$ could contribute to the efficient release and extraction of lignin fragments from lignocellulosic matrix, while an excessive loading of $Fe(OTf)_3$ could lower the delignification degree. Besides, the loading of $Fe(OTf)_3$ mainly influenced the conversion of lignin and xylan instead of glucan.

3.5 Proposed mechanism of metal triflates and Pt/C-involved depolymerization and hydrogenation of lignin

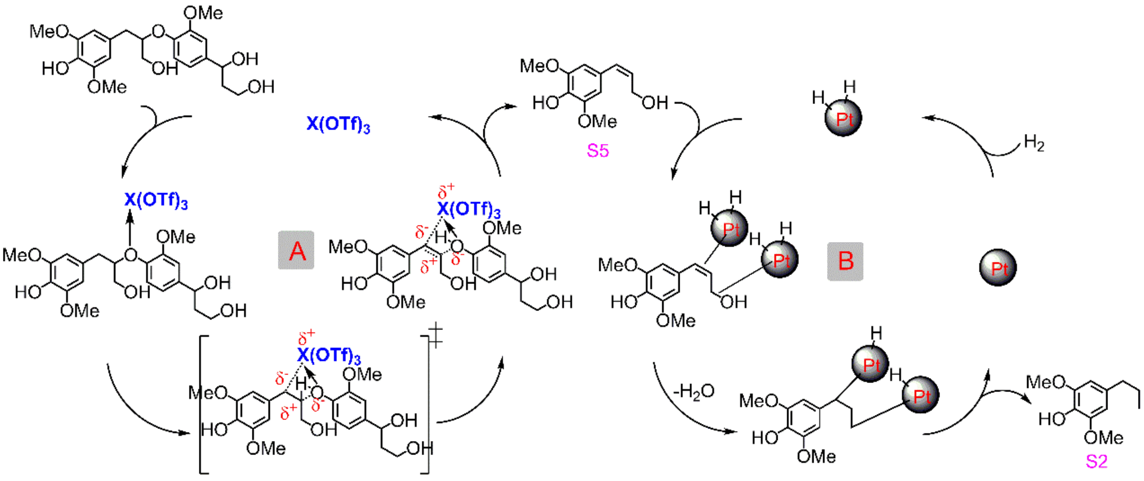

Scheme 1. Proposed reaction pathway of the metal triflates and Pt/C-involved depolymerization and hydrogenation of lignin

The possible mechanism of the delignification, depolymerization of lignin and further stabilization (hydrogenation) of the intermediates is proposed in Scheme 1.

The one-pot process consists of a tandem system in which metal triflates participate in the cleavage of C-O-C ether bonds to form an alkenol intermediate (sinapyl alcohol, S5/coniferyl alcohol) (Cycle A), which undergo further hydrogenation to form saturated propyl syringol (S2) promoted by Pt/C catalyst (Cycle B) (Assary et al., 2013; Atesin et al., 2012; Lohr et al., 2015; Renders et al., 2018). During the two cycles, cycle A involving the C-O-C bond scission was regarded as the rate-determining step with the rate being first-order in terms of substrate and the loading of $Fe(OTf)_3$ (Assary et al., 2013). In the cycle B, the hydrogenation/hydrogenolysis process was dependent on hydrogen pressure (Renders et al., 2018). During the tandem catalytic process, the essential role of Pt/C catalyst involves the decomposition of methanol to produce hydrogen as well as further hydrogenolysis of lignin fragments and hydrogenation of unsaturated monophenolic compounds (Lin et al., 2017; Ouyang et al., 2019). The selectivity toward saturated propyl-substituted phenols (G2+S2) revealed that the hydrogenation of the intermediates was limited since there is no external hydrogen sealed in the reaction system. The proposed pathway was in accordance with the fact that S5 was the major product without the addition of Pt/C (Table 2). An enhanced yield from 10.5 wt% to 32.9 wt% was observed when $Fe(OTf)_3$ was added, which further substantiated the proposed metal triflates-induced C-O-C bond cleavage.

4. Conclusions

In summary, $Fe(OTf)_3$-promoted delignification and microwave-assisted catalytic depolymerization of lignin in birch sawdust in H_2O/MeOH co-solvent without external hydrogen was reported. Among the selected metal triflates, the highest yield of monophenolic compounds of 32.9 wt% was achieved when 0.0276 g of $Fe(OTf)_3$

was added (190 °C, 1 h). The delignification degree also increased from 32.6 wt% to 47.5 wt%, while simultaneously the conversion of hemicellulose rose from 13.3 wt% to 59.6 wt% with furfural and xylose being the major hemicellulose-derived products. The proposed mechanism demonstrated that Lewis acid primarily participated in the scission of ether linkages while Pt/C catalyst contributed to the further hydrogenation of unstable intermediates with C=C bonds. This work provides an efficient Lewis acid-induced delignification and production of monophenolic compounds at relatively mild conditions, which could promote the advancement of “lignin-first” biorefinery strategy.

Declaration of Competing Interest

The authors report no declarations of interest.

Acknowledgements

This work was financially supported by the National Natural Science Foundation of China (No. 21536007), the 111 project (No. B17030) and the Industrial Biotechnology Catalyst (Innovate UK, BBSRC, EPSRC) to support the translation, development and commercialization of innovative industrial Biotechnology processes (EP/N013522/1). X. Liu acknowledges the support from Doctoral Graduate Student’s Academic Visit Project of Sichuan University.

References

Abu-Omar, M.M., Barta, K., Beckham, G.T., Luterbacher, J., Ralph, J., Rinaldi, R., Roman-Leshkov, Y., Samec, J., Sels, B., Wang, F., 2021. Guidelines for performing lignin-first biorefining. Energy Environ. Sci. 14, 262-292.

Assary, R.S., Atesin, A.C., Li, Z., Curtiss, L.A., Marks, T.J., 2013. Reaction Pathways and Energetics of Etheric C–O Bond Cleavage Catalyzed by Lanthanide Triflates. ACS Catal. 3, 1908-1914.

Atesin, A.C., Ray, N.A., Stair, P.C., Marks, T.J., 2012. Etheric C-O bond hydrogenolysis using a tandem lanthanide triflate/supported palladium nanoparticle catalyst system. J. Am. Chem. Soc. 134, 14682-14685.

Bosch, S.V.d., Schutyser, W., Vanholme, R., Driessen, T., Koelewijn, S.F., Renders, T., De Meester, B., Huijgen, W.J.J., Dehaen, W., Courtin, C.M., Lagrain, B., Boerjan, W., Sels, B.F., 2015. Reductive lignocellulose fractionation into soluble lignin-derived phenolic monomers and dimers and processable carbohydrate pulps. Energy Environ. Sci. 8, 1748-1763.

Bouxin, F.P., Clark, J.H., Fan, J., Budarin, V., 2019. Combining steam distillation with microwave-assisted pyrolysis to maximise direct production of levoglucosenone from agricultural wastes. Green Chem. 21, 1282-1291.

Cao, Y., Zhang, C., Tsang, D.C.W., Fan, J., Clark, J.H., Zhang, S., 2020. Hydrothermal Liquefaction of Lignin to Aromatic Chemicals: Impact of Lignin Structure. Ind. Eng. Chem. Res. 59, 16957-16969.

Cederholm, L., Xu, Y., Tagami, A., Sevastyanova, O., Odelius, K., Hakkarainen, M., 2020. Microwave processing of lignin in green solvents: A high-yield process to narrow-dispersity oligomers. Ind. Crops Prod. 145, 112152.

Chen, L., Elias, W.C., Ben Yin, Y., Conrad Zhang, Z., Wong, M.S., 2020a. Acid-catalyzed pyrolytic synthesis of levoglucosan through salt-mediated ring locking. Green Chem. 22, 1968-1977.

Chen, Z., Ragauskas, A., Wan, C., 2020b. Lignin extraction and upgrading using deep eutectic solvents. Ind. Crops Prod. 147, 112241.

Cooreman, E., Vangeel, T., Van Aelst, K., Van Aelst, J., Lauwaert, J., Thybaut, J.W., Van den Bosch, S., Sels, B.F., 2020. Perspective on Overcoming Scale-Up Hurdles for the Reductive Catalytic Fractionation of Lignocellulose Biomass. Ind. Eng. Chem. Res. 59, 17035-17045.

Deuss, P.J., Barta, K., 2016. From models to lignin: Transition metal catalysis for selective bond cleavage reactions. Coord. Chem. Rev. 306, 510-532.

Deuss, P.J., Lahive, C.W., Lancefield, C.S., Westwood, N.J., Kamer, P.C.J., Barta, K., de Vries, J.G., 2016. Metal Triflates for the Production of Aromatics from Lignin. ChemSusChem 9, 2974-2981.

Deuss, P.J., Lancefield, C.S., Narani, A., de Vries, J.G., Westwood, N.J., Barta, K., 2017. Phenolic acetals from lignins of varying compositions via iron(iii) triflate catalysed depolymerisation. Green Chem. 19, 2774-2782.

Deuss, P.J., Scott, M., Tran, F., Westwood, N.J., de Vries, J.G., Barta, K., 2015. Aromatic monomers by in situ conversion of reactive intermediates in the acid-catalyzed depolymerization of lignin. J. Am. Chem. Soc. 137, 7456-67.

Haq, I., Mazumder, P., Kalamdhad, A.S., 2020. Recent advances in removal of lignin from paper industry wastewater and its industrial applications - A review. Bioresour. Technol. 312, 123636.

Huang, X., Gonzalez, O.M.M., Zhu, J., Korányi, T.I., Boot, M.D., Hensen, E.J., 2017. Reductive fractionation of woody biomass into lignin monomers and cellulose by tandem metal triflate and Pd/C catalysis. Green Chem. 19, 175-187.

Huang, X., Zhu, J., Koranyi, T.I., Boot, M.D., Hensen, E.J., 2016. Effective Release of Lignin Fragments from Lignocellulose by Lewis Acid Metal Triflates in the Lignin-First Approach. ChemSusChem 9, 3262-3267.

Jastrzebski, R., Constant, S., Lancefield, C.S., Westwood, N.J., Weckhuysen, B.M., Bruijnincx, P.C., 2016. Tandem Catalytic Depolymerization of Lignin by Water‐Tolerant Lewis Acids and

Rhodium Complexes. ChemSusChem 9, 2074-2079.

Klein, I., Marcum, C., Kenttämaa, H., Abu-Omar, M.M., 2016. Mechanistic investigation of the Zn/Pd/C catalyzed cleavage and hydrodeoxygenation of lignin. Green Chem. 18, 2399-2405.

Kumar, N., Muley, P.D., Boldor, D., Coty, G.G., Lynam, J.G., 2019. Pretreatment of waste biomass in deep eutectic solvents: Conductive heating versus microwave heating. Ind. Crops Prod. 142, 111865.

Lan, W., Luterbacher, J.S., 2019a. Preventing Lignin Condensation to Facilitate Aromatic Monomer Production. Chimia 73, 591-598.

Lan, W., Luterbacher, J.S., 2019b. Preventing Lignin Condensation to Facilitate Aromatic Monomer Production. Chimia (Aarau) 73, 591-598.

Li, C., Zhao, X., Wang, A., Huber, G.W., Zhang, T., 2015. Catalytic Transformation of Lignin for the Production of Chemicals and Fuels. Chem. Rev. 115, 11559-11624.

Li, H., Riisager, A., Saravanamurugan, S., Pandey, A., Sangwan, R.S., Yang, S., Luque, R., 2017. Carbon-Increasing Catalytic Strategies for Upgrading Biomass into Energy-Intensive Fuels and Chemicals. ACS Catal. 8, 148-187.

Liao, Y., Koelewijn, S.-F., Van den Bossche, G., Van Aelst, J., Van den Bosch, S., Renders, T., Navare, K., Nicolaï, T., Van Aelst, K., Maesen, M., 2020. A sustainable wood biorefinery for low–carbon footprint chemicals production. Science 367, 1385-1390.

Lin, L., Zhou, W., Gao, R., Yao, S., Zhang, X., Xu, W., Zheng, S., Jiang, Z., Yu, Q., Li, Y.W., Shi, C., Wen, X.D., Ma, D., 2017. Low-temperature hydrogen production from water and methanol using Pt/alpha-MoC catalysts. Nature 544, 80-83.

Liu, X., Bouxin, F.P., Fan, J., Budarin, V.L., Hu, C., Clark, J.H., 2020a. Microwave-assisted catalytic depolymerization of lignin from birch sawdust to produce phenolic monomers utilizing a hydrogen-free strategy. J. Hazard. Mater. 402, 123490.

Liu, X., Bouxin, F.P., Fan, J., Budarin, V.L., Hu, C., Clark, J.H., 2020b. Recent Advances in the Catalytic Depolymerization of Lignin towards Phenolic Chemicals: A Review. ChemSusChem 13, 4296-4317.

Liu, X., Feng, S., Fang, Q., Jiang, Z., Hu, C., 2020c. Reductive catalytic fractionation of lignin in birch sawdust to monophenolic compounds with high selectivity. Mol. Catal. 495, 111164.

Liu, X., Jiang, Z., Feng, S., Zhang, H., Li, J., Hu, C., 2019. Catalytic depolymerization of organosolv lignin to phenolic monomers and low molecular weight oligomers. Fuel 244, 247-257.

Lohr, T.L., Li, Z., Marks, T.J., 2015. Selective Ether/Ester C–O Cleavage of an Acetylated Lignin Model via Tandem Catalysis. ACS Catal. 5, 7004-7007.

Ouyang, X., Huang, X., Zhu, J., Boot, M.D., Hensen, E.J.M., 2019. Catalytic Conversion of Lignin in Woody Biomass into Phenolic Monomers in Methanol/Water Mixtures without External Hydrogen. ACS Sustain. Chem. Eng. 7, 13764-13773.

Parsell, T., Yohe, S., Degenstein, J., Jarrell, T., Klein, I., Gencer, E., Hewetson, B., Hurt, M., Kim, J.I., Choudhari, H., Saha, B., Meilan, R., Mosier, N., Ribeiro, F., Delgass, W.N., Chapple, C., Kenttämaa, H.I., Agrawal, R., Abu-Omar, M.M., 2015. A synergistic biorefinery based on catalytic conversion of lignin prior to cellulose starting from lignocellulosic biomass. Green Chem. 17, 1492-1499.

Ragauskas, A.J., Beckham, G.T., Biddy, M.J., Chandra, R., Chen, F., Davis, M.F., Davison, B.H., Dixon, R.A., Gilna, P., Keller, M., 2014. Lignin valorization: improving lignin processing in the biorefinery. Science 344, 1246843.

Renders, T., Cooreman, E., Van den Bosch, S., Schutyser, W., Koelewijn, S.F., Vangeel, T., Deneyer, A., Van den Bossche, G., Courtin, C.M., Sels, B.F., 2018. Catalytic lignocellulose biorefining in n-butanol/water: a one-pot approach toward phenolics, polyols, and cellulose. Green Chem. 20, 4607-4619.

Renders, T., Van den Bosch, S., Koelewijn, S.F., Schutyser, W., Sels, B.F., 2017. Lignin-first biomass fractionation: the advent of active stabilisation strategies. Energy Environ. Sci. 10, 1551-1557.

Renders, T., Van den Bossche, G., Vangeel, T., Van Aelst, K., Sels, B., 2019. Reductive catalytic fractionation: state of the art of the lignin-first biorefinery. Curr. Opin. Biotechnol. 56, 193-201.

Rinaldi, R., Jastrzebski, R., Clough, M.T., Ralph, J., Kennema, M., Bruijnincx, P.C., Weckhuysen, B.M., 2016. Paving the Way for Lignin Valorisation: Recent Advances in Bioengineering, Biorefining and Catalysis. Angew. Chem., Int. Ed. 55, 8164-8215.

Schutyser, W., Renders, T., Van den Bosch, S., Koelewijn, S.F., Beckham, G.T., Sels, B.F., 2018. Chemicals from lignin: an interplay of lignocellulose fractionation, depolymerisation, and upgrading. Chem. Soc. Rev. 47, 852-908.

Shen, X., Xin, Y., Liu, H., Han, B., 2020. Product ‐ oriented direct cleavage of chemical linkages in lignin: A review. ChemSusChem 13, 4367-4381.

Shu, R., Long, J., Yuan, Z., Zhang, Q., Wang, T., Wang, C., Ma, L., 2015. Efficient and product-controlled depolymerization of lignin oriented by metal chloride cooperated with Pd/C. Bioresour. Technol. 179, 84-90.

Shu, R., Xu, Y., Ma, L., Zhang, Q., Wang, C., Chen, Y., 2018. Controllable production of guaiacols and phenols from lignin depolymerization using Pd/C catalyst cooperated with metal chloride. Chem. Eng. J. 338, 457-464.

Shuai, L., Amiri, M.T., Questell-Santiago, Y.M., Héroguel, F., Li, Y., Kim, H., Meilan, R., Chapple, C., Ralph, J., Luterbacher, J.S., 2016. Formaldehyde stabilization facilitates lignin monomer production during biomass depolymerization. Science 354, 329-333.

Shuai, L., Saha, B., 2017. Towards high-yield lignin monomer production. Green Chem. 19, 3752-3758.

Sun, J., Li, H., Xiao, L.-P., Guo, X., Fang, Y., Sun, R.-C., Song, G., 2019. Fragmentation of Woody Lignocellulose into Primary Monolignols and Their Derivatives. ACS Sustain. Chem. Eng. 7, 4666-4674.

Sun, Z., Fridrich, B., de Santi, A., Elangovan, S., Barta, K., 2018. Bright Side of Lignin Depolymerization: Toward New Platform Chemicals. Chem. Rev. 118, 614-678.

Tang, J., Guo, X., Zhu, L., Hu, C., 2015. Mechanistic study of glucose-to-fructose isomerization in water catalyzed by [Al (OH) 2 (aq)]+. ACS Catal. 5, 5097-5103.

Van den Bosch, S., Renders, T., Kennis, S., Koelewijn, S.F., Van den Bossche, G., Vangeel, T., Deneyer, A., Depuydt, D., Courtin, C.M., Thevelein, J.M., Schutyser, W., Sels, B.F., 2017. Integrating lignin valorization and bio-ethanol production: on the role of Ni-Al2O3catalyst pellets during lignin-first fractionation. Green Chem. 19, 3313-3326.

Wang, B., Sun, Y., Sun, R., 2019a. Fractionational and structural characterization of lignin and its modification as biosorbents for efficient removal of chromium from wastewater: a review. J. Leather Sci. Eng. 1, 1-25.

Wang, H., Pu, Y., Ragauskas, A., Yang, B., 2019b. From lignin to valuable products-strategies, challenges, and prospects. Bioresour. Technol. 271, 449-461.

Wang, H., Wang, H., Kuhn, E., Tucker, M.P., Yang, B., 2018. Production of Jet Fuel-Range Hydrocarbons from Hydrodeoxygenation of Lignin over Super Lewis Acid Combined with Metal Catalysts. ChemSusChem 11, 285-291.

Wong, S.S., Shu, R., Zhang, J., Liu, H., Yan, N., 2020. Downstream processing of lignin derived feedstock into end products. Chem. Soc. Rev. 49, 5510-5560.

Xu, C., Arancon, R.A., Labidi, J., Luque, R., 2014. Lignin depolymerisation strategies: towards valuable chemicals and fuels. Chem. Soc. Rev. 43, 7485-500.

Yan, J., Meng, Q., Shen, X., Chen, B., Sun, Y., Xiang, J., Liu, H., Han, B., 2020. Selective valorization of lignin to phenol by direct transformation of Csp2–Csp3 and C–O bonds. Sci. Adv. 6, eabd1951.

Yu, I.K.M., Tsang, D.C.W., Yip, A.C.K., Chen, S.S., Ok, Y.S., Poon, C.S., 2016. Valorization of food waste into hydroxymethylfurfural: Dual role of metal ions in successive conversion steps. Bioresour. Technol. 219, 338-347.

Yunden, G., Kano, N., Kim, H.-J., 2019. The Removal of Cr (III) from Aqueous Solution Using Modified Wool. J. Chem 13, 55-61.

Zhao, P., Cui, H., Zhang, Y., Zhang, Y., Wang, Y., Zhang, Y., Xie, Y., Yi, W., 2018. Synergetic Effect of Bronsted/Lewis Acid Sites and Water on the Catalytic Dehydration of Glucose to 5-Hydroxymethylfurfural by Heteropolyacid-Based Ionic Hybrids. ChemistryOpen 7, 824-832.

Zhao, P., Zhou, C., Li, J., Xu, S., Hu, C., 2019. Synergistic Effect of Different Species in Stannic Chloride Solution on the Production of Levulinic Acid from Biomass. ACS Sustain. Chem. Eng. 7, 5176-5183.

Zhou, H., Wang, H., Perras, F.A., Naik, P., Pruski, M., Sadow, A.D., Slowing, I.I., 2020. Two-step conversion of Kraft lignin to nylon precursors under mild conditions. Green Chem. 22, 4676-4682.